Dependence of Optical Properties of Oligo-*para*-phenylenes on Torsional Modes and Chain Length

Vladimír Lukeš,*,† Adélia Justina Aguiar Aquino,‡,§ Hans Lischka,*,‡ and Harald-Friedrich Kauffmann#

Department of Chemical Physics, Slovak University of Technology, Radlinského 9, SK-81 237 Bratislava, Slovakia, Institute for Theoretical Chemistry, University of Vienna, Währingerstrasse 17, A-1090 Wien, Austria, Institute of Soil Research, University of Natural Resources and Applied Life Sciences Vienna, Peter-Jordan-Strasse 82b, A-1190 Vienna, Austria, and Institute for Physical Chemistry, University of Vienna, Währingerstrasse 42, A-1090 Wien, Austria

Received: December 11, 2006; In Final Form: May 4, 2007

A systematic characterization of excited-state properties of *para*-phenylene oligomers constructed from two to eight aromatic rings is presented using density functional theory (DFT) and the coupled-cluster singles and doubles (CC2) method. Geometry optimizations have been performed for the ground state and for the electronically excited state. Vertical excitations and the fluorescence transitions have been calculated. Time-dependent DFT (TDDFT) method underestimates excitation and fluorescence energies systematically in comparison with experimental results. The computed TDDFT lifetime for the polymer limit (0.43 ns) is in agreement with the experimental value of 0.55 ns. The TDDFT torsional potential curves were investigated for biphenyl, terphenyl, and quarterphenyl oligomers in their electronic ground and excited states. Our calculations show an increase in the separation of the lowest excited state (S_1) to the next higher one with increasing molecular size. No indication is found for state crossings of the S_1 state with higher ones from planar structures up to torsional angles of 60° to 70°. Thus, an adiabatic description of the dynamics of the S_1 state might significantly simplify any dynamics simulations of torsional broadenings.

1. Introduction

Conjugated polymers such as *para*-phenylenes are the starting point for the development of very promising organic materials to be used for a variety of applications in electronic and photoelectronic devices. They are unique concerning their high stability and optical properties.[1−4] Whereas the polymeric structures are obtained as highly amorphous materials, their oligomers are of particular interest due to their relatively well-defined structure and easier manipulation, for example, in terms of solubility, purification, and film preparation.[5,6] Short molecules such as *para*-terphenyl ($N = 3$) and *para*-quarterphenyl ($N = 4$) are directly used as laser dyes[7] while the larger *para*-sexiphenyl ($N = 6$) is incorporated in light-emitting diodes.[8]

The electrical and optical properties of most organic molecules with promising technological usage are directly related to the intramolecular delocalization of the π orbitals.[9] The extent of delocalization depends on the size of the overlap between π orbitals of the carbon atoms forming the inter-ring bonds and is therefore governed by the torsional motions around these bonds. The degree of planarity in the polymer ensemble thus directly determines the effective conjugation lengths and, upon coherent electronic femtosecond (fs) excitation, the initial coherence lengths of the (distributed) sites along the physical contour length of the flexible polymer. The occurrence of ultrafast site-structural relaxation caused by the quasi-instantaneous excitation has been demonstrated by femtosecond-wavepacket fluorescence interference experiments.[10] Low-energy, torsional/vibrational background modes coupled to intersite excitation levels set the stage for the dephasing of interstate sites, thereby triggering the generation of relaxed populations (site localization, delocalization shrinking) in a new, nuclear site equilibration. Knowledge of the torsional potentials in the electronic ground state, but most of all, in the excited states is a prerequisite for detailed molecular dynamics simulations on mode couplings and dephasing effects. In this work, the quantum chemical calculation of these potentials and corresponding excited-state geometry optimizations for the *p*-oligophenylenes are intended to prepare the particulars and details for dynamic investigations in subsequent work.

Many theoretical studies on equilibrium geometries of *para*-biphenyl in its electronic ground state have been published.[11−16] Full geometry optimization at the Hartree−Fock level (using 6-311++G(d,p) and smaller basis sets) gives a dihedral angle between 46° and 48°.[11,12,14] The inclusion of correlation effects at the Møller−Plesset perturbation theory to second-order (MP2) level leads to values between 42° and 46°.[11] On the other hand, application of the density functional theory (DFT) method results in smaller dihedral angles (from 39° to 43°).[12,14] It seems that the best MP2 and DFT results are located within the experimental error range obtained for the gas phase (44.4° ± 1.2°).[17]

The situation in liquid and especially in solid-state systems is more complicated. Generally, in the solid phase, the oligomeric structures planarize (dihedral angles starting from 2° to 15°[18−21]). This fact is also reflected in smaller excitation energies in the absorption spectra obtained for films and crystals

* To whom correspondence should be addressed. E-mail: vladimir.lukes@stuba.sk; hans.lischka@univie.ac.at.
† Department of Chemical Physics, Slovak University of Technology.
‡ Institute for Theoretical Chemistry, University of Vienna.
§ Institute of Soil Research, University of Natural Resources and Applied Life Sciences Vienna.
# Institute for Physical Chemistry, University of Vienna.

10.1021/jp068496f CCC: $37.00
Published on Web 06/26/2007

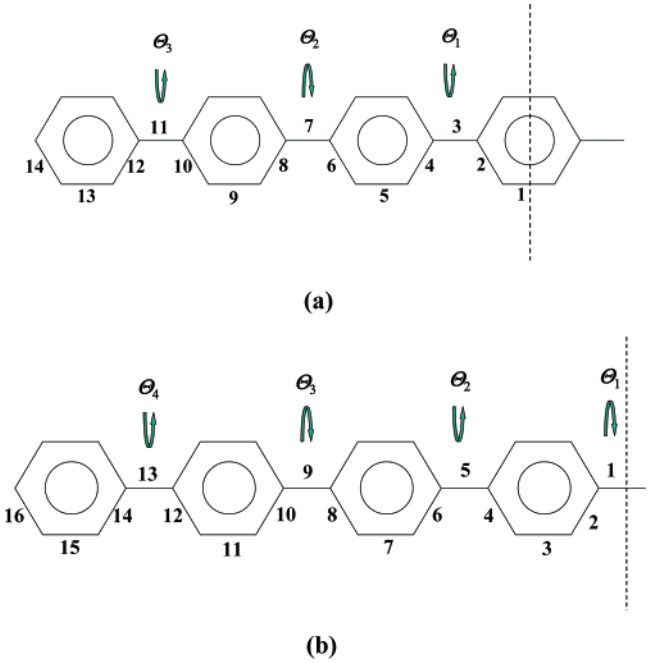

Figure 1. Structure and numbering scheme of studied phenylene-based oligomers for (a) C_{2h} ($N = 7$) and (b) D_2 ($N = 8$) symmetries.

in comparison with solvent measurements.[22,23] Recently, the theoretical characterization of *para*-phenylene oligomers (from dimer to octamer) has been performed at the B3LYP/6-31G* level, and their absorption spectra were calculated at the semiempirical ZINDO/S level.[24] The geometric deformations taking place upon electronic excitation in *p*-terphenyl have been computed by Heimel et al.[25] They have employed a configuration interaction scheme with single excitations (CIS) on top of a Hartree−Fock calculation.

The calculation of electronically excited states is still a very challenging task, especially if one wants to go beyond vertical excitations and compute geometry relaxation effects in excited states. One of the most popular methods is certainly the density functional (DFT) approach and its time-dependent (TD) extension for excited states. Major methodological progress has been achieved by the variational formulation of the TDDFT method by Furche and Ahlrichs,[26] which facilitates the calculation of analytic TDDFT gradients and thus allows for geometry optimizations in excited states. In spite of the overwhelming success of DFT, one should not forget its shortcomings, which led to the development of a large number of functionals. The approximate coupled-cluster singles and doubles method (CC2)[27] is a very interesting alternative. The recent introduction of linear response theory in combination with analytic gradients[28] provides the required possibilities for the treatment of excited states. The implementation of the resolution of the identity (RI) method[29] allows for the efficient treatment of larger molecules. These computational possibilities have been recently used in systematic comparisons between TDDFT and RI-CC2 calculations for oligo-fluorenes[30]—conjugated phenyl rings bridged by CH_2 groups so as to inhibit inter-ring torsional motion. A theoretical investigation of spectral broadening on UV absorption and fluorescence spectra due to the torsional motion using the TDDFT method has been performed for the biphenyl molecule.[31]

In this work, we will focus our attention on the calculation of torsional motions responsible for broadening in absorption and fluorescence spectra of *para*-phenylene oligomers containing 2−8 phenyl rings (see Figure 1). In the spirit of the description of different quantum chemical methods given above, we will use the TDDFT and RI-CC2 methods for the calculation of optimized electronic ground-state and lowest-excited-state geometries. Through the use of these geometries, vertical excitations will be calculated by means of several methods (TDDFT, RI-CC2, and ZINDO/S). The RI-CC2 method (about 10 or 100 times more computationally demanding than TDDFT or ZINDO/S methods, respectively) will be used as much as possible for reference purposes. Subsequently, the computed spectral characteristics will be compared with available experimental data obtained in solution. Finally, an extrapolation to infinite chain length will be performed to obtain the polymer excitation and fluorescence energy limits. Detailed insight into the torsional potential curves in ground and excited states will be presented for *p*-biphenyl, *p*-terphenyl, and *p*-quarterphenyl oligomers.

2. Computational Details

The ground-state and the lowest singlet excited-state geometries of the *para*-phenylene oligomers were optimized at the RI-CC2[28,29] and at the DFT and TDDFT[26,32,33] levels, respectively, using the B3LYP functional.[34] Geometry optimizations were restricted to D_2 symmetry for molecules with an even number ($N = 2$, 4, 6, and 8) of aromatic rings and to C_{2h} symmetry for molecules with an odd ($N = 3$, 5, and 7) number of aromatic rings. Due to the large number of possible orientations of dihedral angles, only the all-anti conformations were investigated (see orientations of dihedral angles Θ_i in Figure 1). The molecules were oriented in such a way that the torsional axis coincides with the *z*-axis. On the basis of the optimized geometries, the electronic absorption and fluorescence spectra were calculated at the RI-CC2, TDDFT, and the ZINDO/S[35] levels. Vertical excitations are computed at the ground-state geometry. The fluorescence transition is obtained as the vertical de-excitation at the optimized geometry of the energetically lowest excited state with dominant oscillator strength. For the ZINDO/S calculations, the TDDFT geometries were used and the single excitations from the 15 highest occupied (HOMO) to the 15 lowest unoccupied molecular orbitals (LUMOs) were considered. The polarized split-valence SVP and SV(P)[36] and the triple-ζ valence-polarized (TZVP)[37] basis sets have been used for the geometry optimization and/or spectral calculations. In the case of RI-CC2 calculations, we have also augmented the SVP basis set by a set of diffuse functions whose exponents have been obtained from the lowest s, p, and d exponents by division of a factor of 3 (denoted as SVP+). All calculations were done using the Turbomole[38] and Hyperchem (ZINDO/S calculations)[39] program packages.

3. Results and Discussion

A. Ground-State Structures and Vertical Excitation Energies. The oligomer structures and the atomic numbering scheme are depicted in Figure 1. Optimized bond lengths for the electronic ground state obtained at the DFT and CC2 levels are visualized in Figure 2. The smallest C−C bond distances are located in the central part of the phenylene rings (see bonds 3, 7, 11, and 15 for $N = 2$, 4, 6, 8 and nos. 1, 5, 9, and 13 for $N = 3$, 5, 7). The largest bond lengths are found for the inter-ring distances (see bond nos. 1, 5, 9, and 13 for $N = 2$, 4, 6, 8 and nos. 3, 7, and 11 for $N = 3$, 5, 7). The B3LYP/SVP distances between the phenylene rings are in most cases slightly shorter (about 0.003 Å) than the ones obtained with the RI-CC2/SV(P) approach. The elongation of the molecular chain leads only to small changes in these inter-ring distances. The

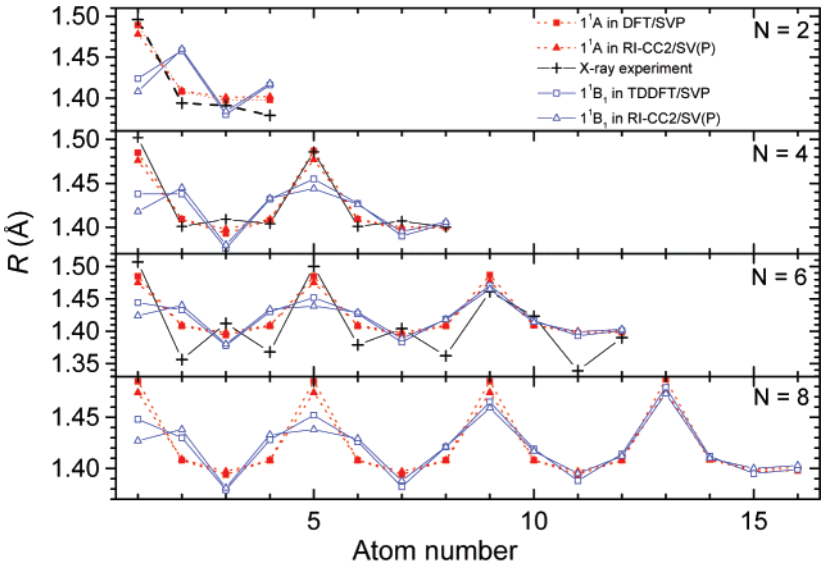

(a)

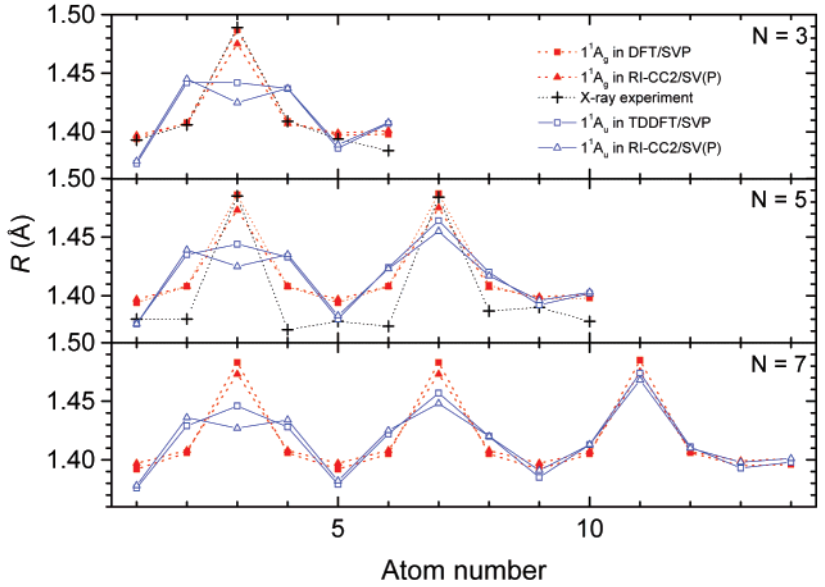

(b)

Figure 2. Experimental[16−19] and computed C−C bond lengths of the studied oligomers with (a) even (N = 2, 4, 6, 8) and (b) odd (N = 3, 5, 7) numbers of repeat units for the electronic ground states (1^1A or 1^1A_g) and the excited states 1^1B_1 or 1^1A_u. See Figure 1 for bond numbering.

largest change occurs for a terminal ring becoming an inner one. After further extension, the bond-length differences seem to by quite well converged. For the sake of comparison, C−C bond lengths obtained from X-ray measurements[17] are included in Figure 2. Comparison with these values helps us to estimate the environmental effects on the individual bonds. It seems that the most sensitive positions are located at side C−C bonds within phenylene rings (e.g., see bond nos. 2, 4, 6, 8 for N = 5 and 6).

The dependence of the dihedral angles on the number of phenylene rings is depicted in Figure 3. For biphenyl, the B3LYP/SVP dihedral angle between the rings is about 37° whereas the RI-CC2/ SV(P) method gives a value of 45°, which agrees well with the experimental gas-phase value of 44.4°.[17] In almost all cases, the torsional angles decrease slightly with oligomer lengths and the torsion in the central parts of the oligomer is smaller by about 1° than that at the ends (e.g., see angles for N = 7 and N = 8). Available crystal structures for N = 2−6 indicate more planar inter-ring torsion angles (e.g., 2° for biphenyl[18]).

The vertical excitation energies calculated at the TDDFT/SVP and RI-CC2/ SV(P) levels based on corresponding optimized geometries are collected in Table 1. Both methods used indicate dominant oscillator strengths for the 1^1B_1 (N = 2, 4, 6, and 8) and 1^1A_u (N = 3, 5, and 7) electronic states. Non-negligible differences in the ordering of states in the TDDFT and RI-CC2 calculations are observed. For example, RI-CC2 calculations give the 1^1B_3 state as the second lowest excited state for the biphenyl molecule (5.02 eV). The 1^1B_1 state is the third-highest state with excitation energy of 5.75 eV. Our major concern is the investigation of the spectroscopically bright state. It is important to note that there is agreement between

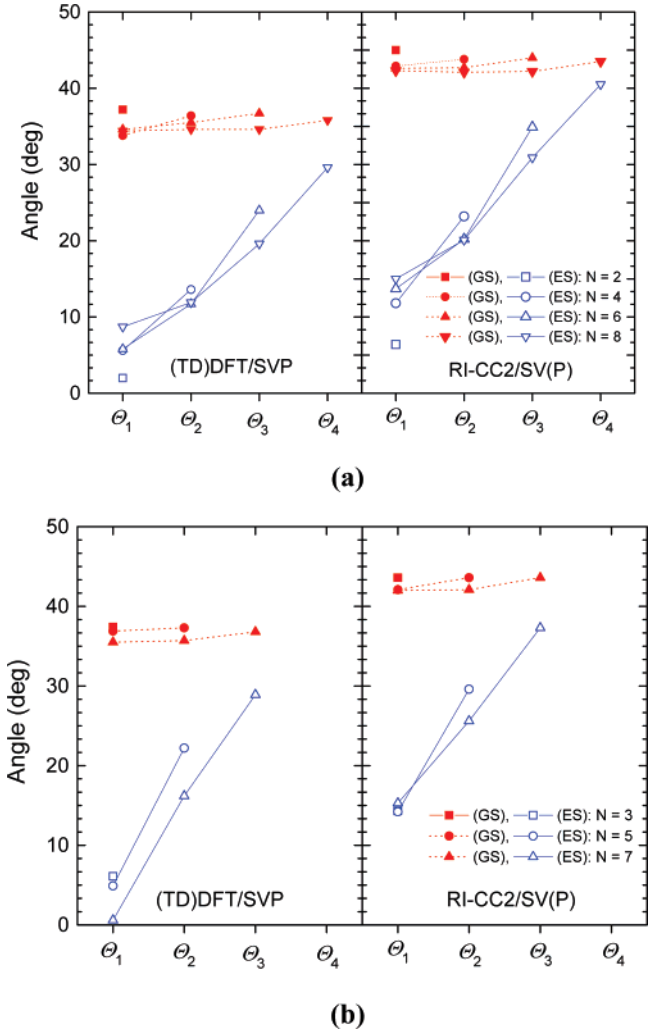

Figure 3. Optimized interring dihedral angles Θ_i of the studied oligomers with (a) even ($N = 2, 4, 6, 8$) and (b) odd ($N = 3, 5, 7$) numbers of repeat units for the electronic ground (GS) 1^1A or 1^1A_g (solid symbols) and the excited states (ES) 1^1B_1 or 1^1A_u (open symbols). See Figure 1 for angle numbering.

the two methods based on the fact that this state is the lowest one for the larger oligomers and that its separation to the next higher states increases with chain length. These findings will be discussed below in connection with computed torsional potential curves.

The differences in the ordering of states between the TDDFT and RI-CC2 calculations is certainly not of big relevance for the absorption spectrum for intensity reasons, as mentioned above. The experimental UV−vis absorption spectra of *p*-oligophenylenes indicate broad and structureless bands. Due to the importance of the 1^1B_1 and 1^1A_u states discussed above, the shape of these bands should be explained by transitions to these states broadened by torsional inter-ring modes (see ref 31) and environmental effects.

In Table 1S (see Supporting Information) and Figure 4, we present the dependence of the excitation energy of the 1^1B_1 and 1^1A_u states, respectively, on the chain length of the oligomer series. All excitation energies decrease with the elongation of the chain and display good linear dependence (regression coefficients are better than 0.996) on the inverse number of repeat units ($1/N$). For example, the addition of two phenylene rings to biphenyl leads to a decrease in the excitation energy of the 1^1B_1 state by about 0.9 eV (see SVP results in Table 1S). In the TDDFT, the deviation from experiments increases with chain length. The extension of the basis set from SVP to TZVP for B3LYP/SVP geometries decreases TDDFT excitation energies mainly for the smallest oligomers ($N = 2$ and 3) by about 0.1 eV. However, the extrapolated TDDFT limits are identical for the SVP and TZVP basis sets (2.94 ± 0.01 eV). Almost the same value (2.97 eV) published by Ma et al.[40] was obtained from the B3LYP/6-31G(d) study of the first five phenylene oligomers ($N = 1, 5$). A similar underestimation of TDDFT excitation energies was also found for other conjugated chainlike systems.[30] This fact is related to the limitation of the current approximate exchange functionals in correctly describing the exchange-correlation potential in the asymptotic region.[41] On the other hand, the RI-CC2/SV(P) calculations using the RI-CC2/SV(P) geometries give excitation energies which are significantly higher (limit is 3.99 ± 0.01 eV) than the extrapolated experimental energies (3.51 ± 0.05 eV or 3.35 ± 0.05 eV for solution[22,23]). The single-point calculations in RI-CC2/SV(P) geometries using the extended SVP+ basis set led to reductions of the excitation energies by 0.2−0.3 eV (the extrapolated value is 3.82 ± 0.02 eV). A similar overestimation of CC2 results with respect to the experimental data and their basis set sensitivity was recently reported for the oligothiophene series by Fabiano et al.[42] The fit to the RI-CC2 results gives a line, which is well parallel to the one obtained for the experimental data available for a cyclohexane−benzene solution (see Figure 4).[23] In contrast, the TDDFT results give a line that is too steep. Finally, we would like to note that due to the specific parametrization for the π-conjugated aromatic system on their spectroscopic properties, the semiempirical ZINDO/S results (calculated in B3LYP/SVP geometries) are in very good agreement with the above-mentioned experimental values. The extrapolated ZINDO/S limit represents (3.62 ± 0.02 eV) the value near the experimentally determined interval.

To characterize the optical transitions, it is useful to examine the HOMO and the LUMOs because the HOMO−LUMO excitation plays a dominant role. With more than 94%, it contributes to the 1^1B_1 and/or 1^1A_u lowest singlet excited state for $N > 2$ (see Table 1). The HOMO and LUMO of heptaphenyl ($N = 7$) and octaphenyl ($N = 8$) are shown in Figure 5. It is interesting to note that the HOMO and LUMOs are localized in the central part of the molecule. The LUMOs nicely show the inter-ring bonding character, which is also reflected in the shortenings of the corresponding inter-ring C−C distances in the lowest excited state as will be discussed in the next section.

B. Excited-State Geometries and Florescence. The electronic excitation of the studied oligomers leads to formation of a partially quinoid-type structure. The bonds between the phenylene rings are shortened while the adjacent intra-ring bonds are elongated (see RICC2/SV(P) and TDDFT/SVP results in Figure 2). The largest effects are found in the central part of the oligomer for $N < 6$. The planarization of the molecular skeleton is concentrated in the same region of the oligomers (compare dihedral angles between the ground state and excited state for RICC2/SV(P) and TDDFT/SVP results in Figure 3). Similar results were also reported for a unit cell containing 28 phenylene monomers using a constrained DFT method.[42] The structural relaxations in the lowest excited states are largely confined to a region of approximately eight monomers over which the torsional angles and inter-ring bonds are significantly reduced in comparison with the electronic ground state. On the basis of the geometries optimized for the 1^1B_1 and 1^1A_u excited states, the fluorescence spectra were calculated. The dependence of the fluorescence energies on the number of aromatic units is illustrated in Figure 6, and the numerical values for all performed

TABLE 1: Excitation Energies (in electronvolts) Calculated Using TDDFT/SVP and RI-CC2/ SV(P) for Optimized Geometries[a]

	TDDFT /SVP		RI-CC2 /SV(P)			TDDFT /SVP		RI-CC2 /SV(P)	
$N=2$	1^1B_2	4.93	1^1B_2	5.06	$N=3$	1^1A_u	4.30 (0.934)	1^1B_u	4.86
	1^1B_1	4.94 (0.460)	1^1B_3	5.02		1^1B_u	4.67	1^1B_g	5.02
	1^1B_3	5.01	1^1B_1	5.75 (0.583)		1^1B_g	4.84	2^1B_u	5.02
	2^1B_2	5.69 (0.015)	2^1B_2	6.76 (0.065)		2^1B_u	4.87	1^1A_u	5.17 (1.190)
	2^1B_3	5.83 (0.102)	2^1A	6.81		2^1A_g	5.10	2^1A_g	6.14
	2^1A	5.93	2^1B_3	6.89 (0.352)					
$N=4$	1^1B_1	3.95 (1.365)	1^1B_2	4.86	$N=5$	1^1A_u	3.74 (1.727)	1^1A_u	4.67 (2.334)
	1^1B_2	4.54	1^1B_3	4.87		2^1A_g	4.35	1^1B_u	4.81
	2^1A	4.61	1^1B_1	4.89 (1.774)		3^1A_g	4.52	2^1B_u	4.83
	2^1B_3	4.65	2^1B_2	5.06		1^1B_u	4.54 (0.001)	1^1B_g	4.84
	2^1B_2	4.80	2^1B_3	5.06		1^1B_g	4.64	2^1B_g	5.02
	3^1B_3	4.80 (0.001)	2^1A	5.72					
$N=6$	1^1B_1	3.59 (2.044)	1^1B_1	4.57 (2.923)	$N=7$	1^1A_u	3.51 (2.489)	1^1A_u	4.50 (3.488)
	2^1A	4.14	1^1B_2	4.80		2^1A_g	4.04	1^1B_u	4.80
	1^1B_3	4.47	1^1B_3	4.81		3^1A_g	4.10	2^1B_u	4.81
	2^1B_2	4.54	2^1B_2	4.83		2^1A_u	4.45 (0.270)	1^1B_g	4.81
	2^1B_3	4.60	2^1B_3	4.83		3^1A_u	4.46 (0.411)	2^1B_g	4.83
	3^1B_2	4.63	2^1A	5.01					
$N=8$	1^1B_1	3.45 (2.946)	1^1B_1	4.44 (3.845)					
	2^1B_1	4.26 (0.741)	1^1B_2	4.80					
	3^1B_1	4.27 (0.013)	1^1B_3	4.80					
	1^1B_3	4.40	2^1B_2	4.81					
	4^1B_1	4.42 (0.006)	2^1B_3	4.81					
	2^1A	3.90	2^1A	4.82					

[a] Significant oscillator strengths are indicated in parentheses.

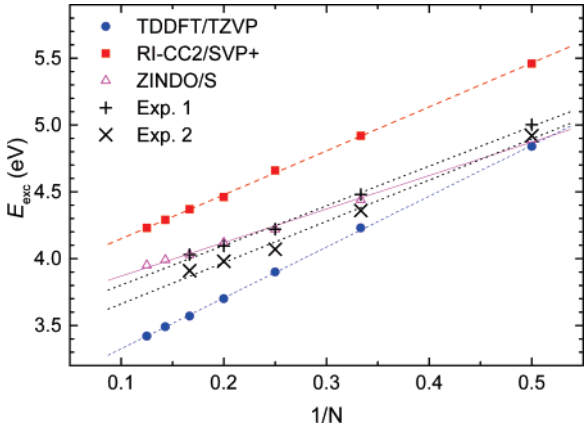

Figure 4. Dependence of the vertical excitation energy to the 1^1B_1 and 1^1A_u states, respectively, on the inverse number of phenylene rings. The experimental data for *para*-oligophenylenes were measured in tetrahydrofurane (expt. 1)[22] and cyclohexane−benzene (expt. 2)[23] solution.

calculations are collected in Table 2S. The asymptotic TDDFT/SVP and TDDFT/TZVP values calculated at TDDFT/ SVP geometries are 2.23 ± 0.01 and 2.21 ± 0.01 eV. These energies are again too low in comparison with experimental values (see below). Almost the same underestimation was obtained from solving the Bethe−Salpeter equation for the excitation of an electron including the electron−hole interaction in solids and polymers.[43] The asymptotic RI-CC2/SV(P) and RI-CC2/SVP+ fluorescence energies are 2.95 ± 0.02 and 2.77 ± 0.01 eV, respectively, and in good agreement with the asymptotic ZINDO/S (2.89 ± 0.02 eV) energy and values measured for the polyphenylenes in different solvents (2.85 ± 0.04 eV for tetrahydrofurane[22] and 3.07 ± 0.05 eV in cyclohexane−benzene mixtures).[23]

To investigate the effects of the structural relaxation upon excitation, a comparison of the slopes for excitation and fluorescence energies vs $1/N$ is of interest. In all cases, the slopes for the fluorescence energies are about 0.2−0.3 eV smaller than those for the excitation energies. These differences should be reflected also in the Stokes shifts. The evaluated Stokes-shift changes computed as the differences $\Delta E = E_{exc} - E_{fl}$ on the inverse number N are included in the inset of Figure 6. The TDDFT/TZVP values exhibit a Stokes shift of about 0.75 eV for $N > 4$ which are lower than the CC2/SVP+ energies by about 0.31 eV. The available experimental data for $N > 4$ measured in solution show a smaller Stokes shift between 0.63 and 0.68 eV.

On the basis of the fluorescence energy and oscillator strength, the radiative lifetimes have been computed for spontaneous emission using the Einstein transition probabilities according to the formula[44]

$$\tau = \frac{c^3}{2(E_{Flu})^2 f} \qquad (1)$$

where c is the velocity of light, E_{Flu} is the transition energy, and f is the oscillator strength.

The computed lifetime τ for biphenyl (see Figure 7) amounts to 1.48 ns for ZINDO/S, 1.73 ns for RI-CC2/SVP+ (in RI-CC2/SV(P) geometry), and 2.47 ns for B3LYP/TZVP (in B3LYP/SVP geometry). The experimental value for the radiative life time is 16 ns. It should be noted that the experimental value is also in considerable contrast to the experimental radiative lifetimes found for the larger oligomers (see below). Good agreement between calculated results and experiment is observed for $N > 2$. The increase in molecular chain leads to a decrease in fluorescence energies and to an increase in oscillator strengths. This results in a decrease in calculated radiative lifetimes. The calculated ZINDO/S (0.36 ± 0.02 ns) and TDDFT/TZVP (0.43 ± 0.02 ns) polymer limits are in good agreement with the experimental value (the result for biphenyl was excluded from the linear regression) of 0.55 ± 0.05 ns for solution. The value of 0.19 ± 0.02 ns for RI-CC2/SVP+ is somewhat lower than the experimental limit.

C. Torsional Potentials for the Electronic Ground and the Lowest Excited State. Torsional potentials were computed for the oligomers with 2, 3, and 4 aromatic rings by changing the torsional angles between adjacent phenylene rings in 10° steps. The geometries were optimized for each setting of dihedral

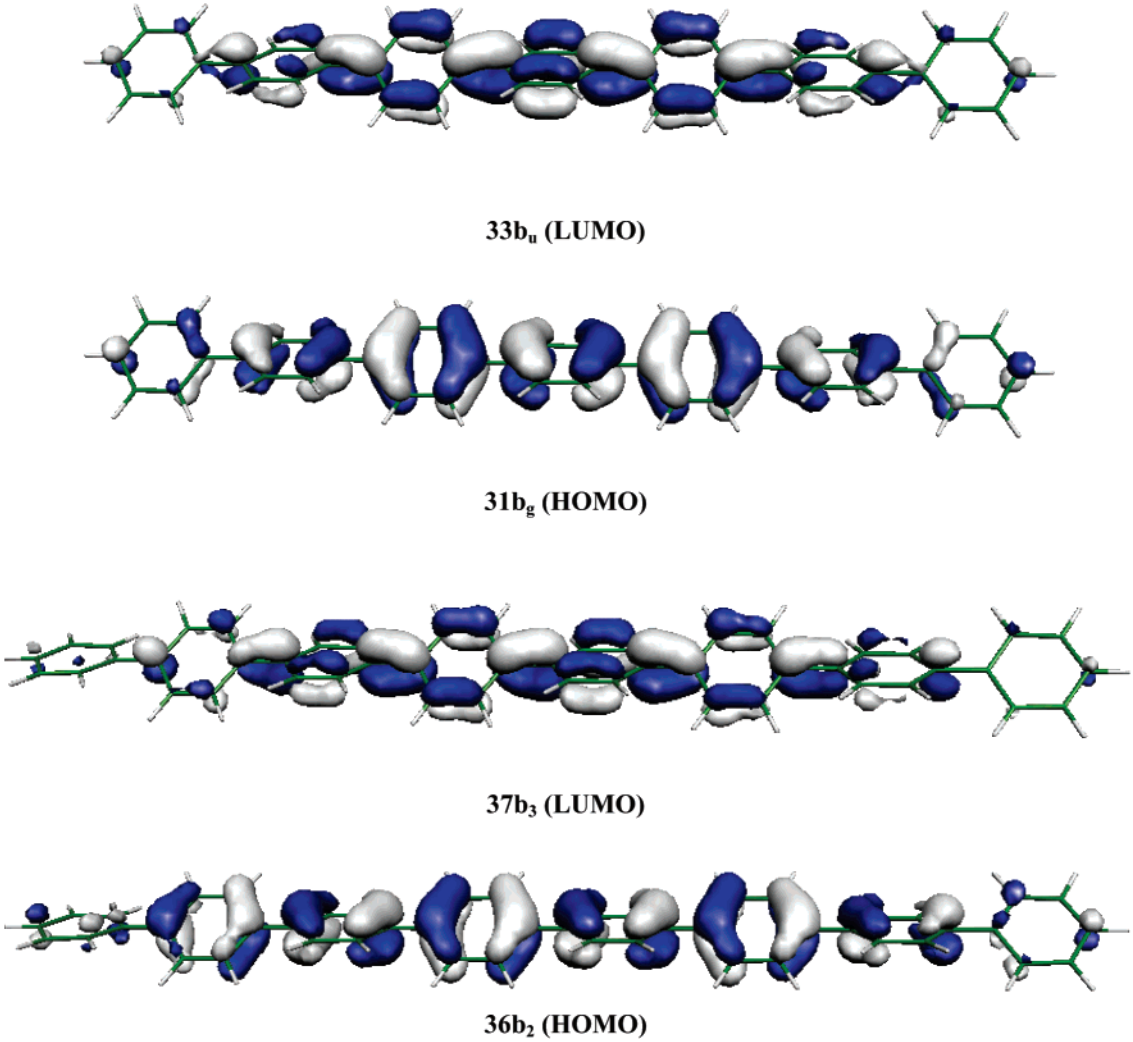

Figure 5. Plots of HOMO and LUMO (calculated at the B3-LYP/SVP level) of oligomers with (a) $N = 7$ and (b) $N = 8$.

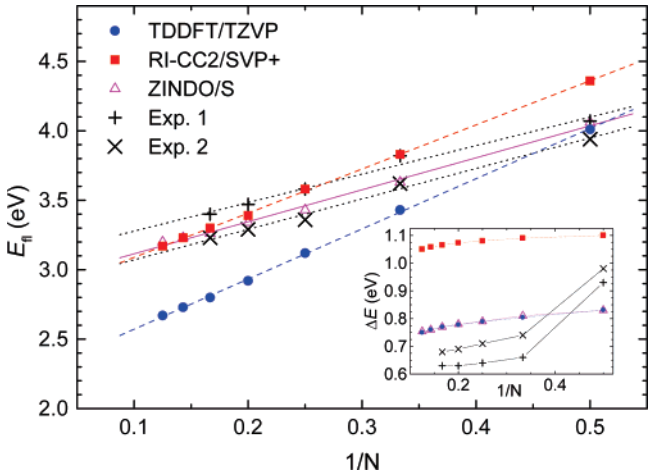

Figure 6. Dependence of the fluorescence energies on the inverse number of phenylene rings (N). The experimental data for *para*-oligophenylenes were measured in tetrahydrofurane (expt. 1)[22] and cyclohexane−benzene (expt. 2)[23] solution (inset: dependence of Stokes-shift changes with $1/N$).

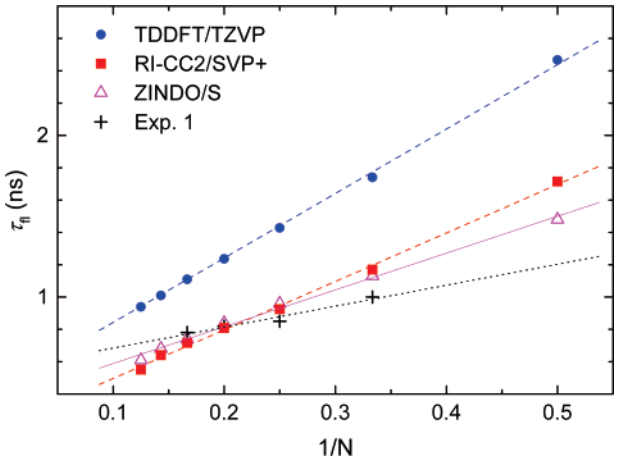

Figure 7. Dependence of the radiative fluorescence lifetimes on the number of phenylene rings. The experimental data for *para*-oligophenylenes were measured in cyclohexane−benzene solution.[23]

angles under the restriction of $|\Theta_1| = |\Theta_2| = |\Theta_3| = |\Theta_4| = \Theta$ (see Figure 1) and corresponding symmetries D_2 or C_{2h}. The computed ground-state torsional potentials of biphenyl, terphenyl, and quarterphenyl molecules using the B3LYP/SVP method are shown in Figure 8. Two barriers are observed in accordance with recently published DFT studies.[11,15,24] As can be seen in Figure 8, for biphenyl the barrier to planarity is smaller (1.53 kcal·mol^{-1}) than that to the perpendicular structure (2.38 kcal·mol^{-1}). Qualitatively similar B3LYP results were reported by Fabiano and Della Sala.[15] They indicated a minimum located at ~40° and barrier heights 1.78 kcal·mol^{-1} for $\Theta =$ 0° and 2.12 kcal·mol^{-1} for $\Theta = 90°$. In the Møller−Plesset perturbation method, up to the second-order (MP2) and coupled-

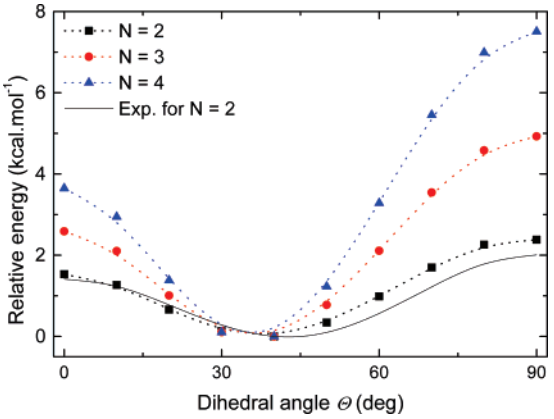

Figure 8. Potential curves ($|\Theta_1| = |\Theta_2| = |\Theta_3| = |\Theta_4| = \Theta$) calculated for the electronic ground state (1^1A, respectively, 1^1A_g) using the TDDFT/SVP method. Energies are given relative to the energy minimum. The solid line indicates the experimentally determined values for the biphenyl molecule.[39]

cluster calculations with single, double, and perturbatively estimated triple excitations (CCSD(T)) exhibit a larger barrier for planar structure. The best current predictions for these two barriers for biphenyl amount to 2.1 (1.7) kcal·mol^{-1} and 2.2 (1.8) kcal·mol^{-1} at the CCSD(T) and MP2 extrapolated levels, respectively.[43] Comparison of the experimentally determined torsional potential[31,46] and our calculated torsional potential for biphenyl reveals good agreement for angles between 0 and 60° (see solid line in Figure 8). The computed barrier for the planar structure is in good agreement with the experimentally deduced value (1.4 kcal·mol^{-1})[44] whereas the perpendicular barrier (2.38 kcal·mol^{-1}) is higher by about 19% with respect to the experimental value (2.00 kcal·mol^{-1}).[46]

The electronic ground-state potential curves for $N = 3$ and $N = 4$ have the same shape as those for $N = 2$ (see Figure 8). However, in the former cases, the barriers heights are about twice as high at the perpendicular conformation in comparison with the planar one. A similar feature was observed from Hartree−Fock calculations for $N = 3$,[25] where the lower energy barrier at 0° is 4.39 kcal·mol^{-1} and at 90° is 8.31 kcal.mol^{-1}. Because of the higher barriers, the larger oligophenylenes are thermally more restricted than in the $N = 2$ case.

Excited-state potential energy curves calculated at the TDDFT/SVP level based on ground-state optimized geometries are shown in Figure 9. The curves for the excited state of 1^1B_1 (for $N = 2$, 4) and 1^1A_u (for $N = 3$) symmetries show an energy minimum for a planar geometry and a maximum for the perpendicular one. In the case of biphenyl, the 1^1B_3 state is close to the 1^1B_1 state at 0°. On the other hand, the curve for the 1^1B_2 state crosses the 1^1B_3 and 1^1B_1 curves at a dihedral angle of 44°. For the perpendicular orientation, the 1^1B_2 and 1^1B_3 states merge to the degenerate 1^1E state for D_{2d} symmetry. A very similar situation has been reported by Beenken and Lischka.[31] The addition of more phenylene rings leads to a larger separation between the two lowest states (1^1B_3 and 1^1B_1 and 1^1A_u and 1^1B_u states, respectively) amounting to 0.4 eV for $N = 3$ and 0.6 eV for $N = 4$ at planar geometry. Moreover, with an increasing number of phenylene rings, the crossing region of potential curves between the two lowest excited states is shifted to higher dihedral angles (around 60° to 70° for $N = 3$ and 4). The potential energy curves for the next higher excited states are quite closely spaced to each other and show multiple intersections.

The potential curves calculated at the TDDFT/SVP level for relaxed 1^1B_1 and 1^1A_u excited-state geometries, respectively,

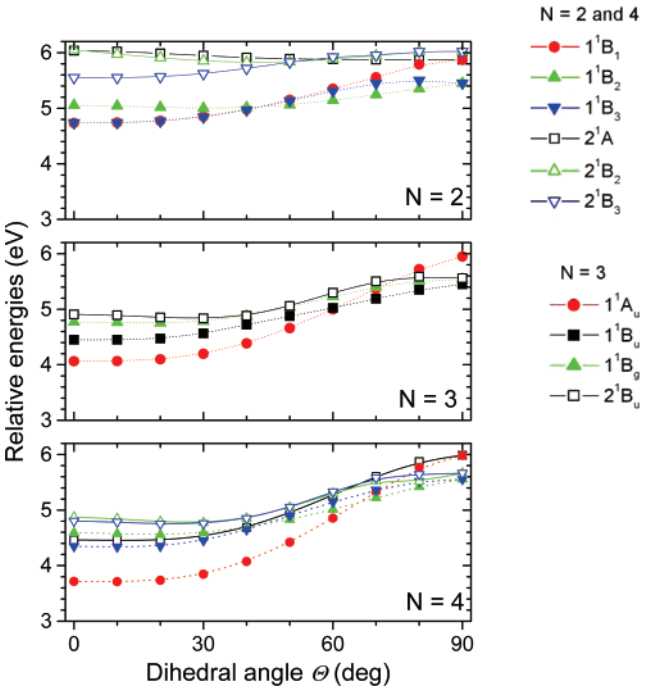

Figure 9. Potential curves ($|\Theta_1| = |\Theta_2| = |\Theta_3| = |\Theta_4| = \Theta$) calculated at the TDDFT/ SVP level for the lowest vertically excited states of biphenyl ($N = 2$), terphenyl ($N = 3$), and quarterphenyl ($N = 4$) using optimized geometries of the ground state. The ground-state energy minimum is taken as the energy reference.

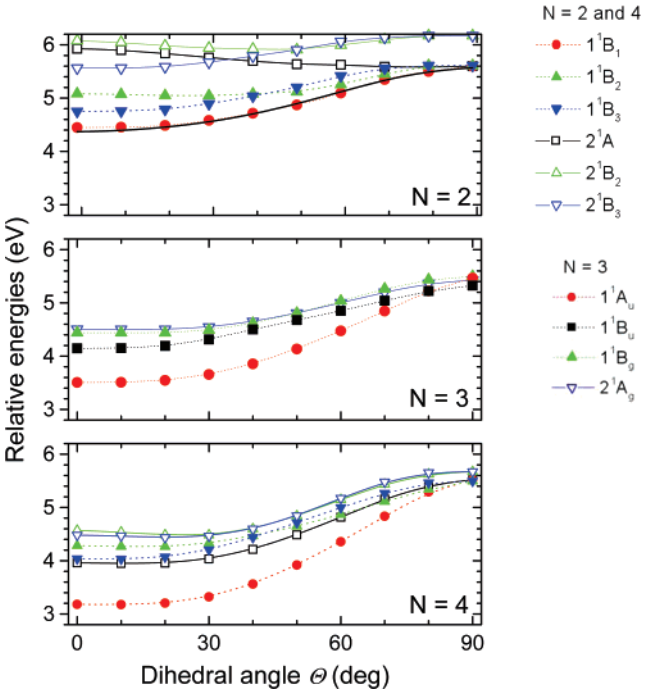

Figure 10. Potential curves ($|\Theta_1| = |\Theta_2| = |\Theta_3| = |\Theta_4| = \Theta$) calculated at the TDDFT/ SVP level for the lowest vertically excited states of biphenyl ($N = 2$), terphenyl ($N = 3$), and quarterphenyl ($N = 4$) using relaxed geometries of the $1^1B_1/1^1A_u$ states. The ground-state energy minimum is taken as the energy reference. The solid line indicates the experimentally determined values for the biphenyl molecule.[46]

are shown in Figure 10. The shape of the potential energy curves for the relaxed, lowest excited states does not differ much in shape from those of the corresponding curves using the ground-state geometries (compare Figures 9 and 10). Primarily, an overall shift of the potential energy curves is observed to lower

energies by 0.4−0.5 eV which is also reflected in the different slopes for dependencies of excitation and fluorescence energies on $1/N$ (see Figures 4 and 6). This fact indicates that the vibrational relaxation is to a good approximation independent of the torsional angle. Even though the B3LYP/SVP calculations are in good agreement with the experimentally determined potential curve of the fluorescent 1^1B_1 state (see the solid line in Figure 10)[46] already, the basis set effect was investigated as well. The extension of the basis set from SVP to TZVP using B3LYP/SVP geometries has a relatively small effect on the individual potential curves. A shift of about 0.1 eV is found for the lowest vertically excited $\mathbf{1^1B_1}$ ($N = 2$ and 4) and $\mathbf{1^1A_u}$ ($N = 3$) potential curves (see data in Table 3S). On the other hand, the basis set sensitivity based on the relaxed geometries of the $1^1B_1/1^1A_u$ states (see data in Table 4S) is even less in comparison with data collected in Table 3S.

4. Conclusions

A systematic theoretical study has been performed on the properties of excited states of *para*-phenylene oligomers up to eight repeat units. Optimized geometries were obtained not only for the electronic ground state but also for the lowest electronically excited state of each system. Because of computational efficiency, B3LYP has been applied for the geometry optimizations of the larger oligomers. The RI-CC2 method was used for selected reference calculations. Electronic excitation leads to quinoid-type distortions, in particular to a shortening of the inter-ring bonds and concomitant planarization of the inner inter-ring torsions. This behavior correlates very well with the nodal properties of the LUMO. Good linear dependence of computed excitation and fluorescence energies was observed with respect to $1/N$ (N is the number of repeat units). TDDFT calculations systematically underestimate excitation and fluorescence energies for larger systems ($N > 4$). RI-CC2 overestimates these quantities. The ZINDO/S method has been applied as well using the optimized B3LYP geometries. The slopes of calculated electronic and fluorescence spectra are in a very good agreement with available experimental results measured in different solutions.

TDDFT torsional potential energy curves in the electronic ground and in the excited states were also investigated in this work for biphenyl ($N = 2$), terphenyl ($N = 3$), and quarterphenyl ($N = 4$) oligomers. Torsional curves were computed using fixed ground-state geometries and relaxed ones based on the optimization of the lowest excited state. The TDDFT curves show an increasing separation of the lowest excited state from the remaining excited states at planar geometries. The torsional potential also becomes significantly steeper with increasing chain length. The barrier to the orthogonal structure increases from 1.14 eV ($N = 2$) to 2.27 eV ($N = 4$). In agreement with the TDDFT results, the RI-CC2 calculations also give the state with the most intense transition ($1^1B_1/1^1A_u$) as the lowest one for larger oligomers sizes. Even though the ordering of the remaining states differs in part considerably from the TDDFT results, the increasing separation of the S_1 state from the higher ones is confirmed. Starting with terphenyl, the S_1 state computed at the TDDFT level also corresponds to the most intense transition. The present investigations show that for oligomers sizes starting with 3−4 repeat units the lowest excited state is the bright state. This state also seems to be well separated from the remaining ones with respect to torsional modes. From our calculations, we do not find any indication of state crossings of the S_1 state with higher ones up to torsional angles of 60°−70°. Thus, it should be possible to perform dynamics simulations of the torsional broadening of absorption and emission spectra based on an adiabatic approach, which will simplify the calculations considerably.

Acknowledgment. The authors acknowledge support by the Austrian Science Fund within the framework of the Project P18233 and Special Research Program F16(18), Advanced Light Sources (ADLIS). The calculations were performed in part on the Schrödinger III cluster of the University of Vienna.

Supporting Information Available: Total electronic energies and fully optimized Cartesian coordinates for studied systems calculated using TDDFT/SVP and RI-CC2/SV(P) are given. Data for Figures 4, 6, 9, and 10 is also given. This material is available free of charge via the Internet at http://pubs.acs.org.

References and Notes

(1) Kiess, H., Ed. *Conjugated Conducting Polymers*; Springer: Berlin, 1992.
(2) André, J. M.; Delhalle, J.; Brédas, J. L. *Quantum Chemistry Aided Design of Organic Polymers. An Introduction to the Quantum Chemistry of Polymers and its Applications*; World Scientific: Singapore, 1991.
(3) Rohlfing, M.; Louie, S. G. *Phys. Rev. Lett.* **1999**, *82*, 1959.
(4) Ahn, K.-H.; Ryu, G. Y.; Yun; S-W.; Shin, D.-M. *Mater. Sci. Eng. C* **2004**, *24*, 163.
(5) Bäuerle, P. In *Electronic Materials: The Oligomer Approach*; Müllen, K., Wegner, G., Eds.; Wiley-VCH: Weinheim, Germany, 1998.
(6) Johansson, N.; Salbeck, J.; Bauer, J.; Weissörtel, F.; Bröms, P.; Andresson, A.; Salaneck, W. R. *Synth. Met.* **1999**, *101*, 405.
(7) Furumoto, H. W.; Ceccon, H. L. *IEEE J. Quantum Electron.* **1970**, *6*, 262.
(8) Koch, N.; Pogantsch, A; List, E. J. W.; Leising, G.; Blyth, R. I. R.; Ramsey, M. G.; Netzer, F. P. *Appl. Phys. Lett.* **1999**, *74*, 2909.
(9) Brédas, J.-L.; Beljonne, D.; Coropceanu, V.; Cornil, J. *Chem. Rev.* **2004**, *104*, 4971.
(10) Milota, F.; Sperling, J.; Szöcs, V.; Tortschanoff, A.; Kauffmann, H. F. *J. Chem. Phys.* **2004**, *120*, 9870.
(11) Grein, F. *J. Mol. Struct. THEOCHEM* **2003**, *624*, 23.
(12) Karpfen, A.; Choi, C. H.; Kertesa, M. *J. Phys. Chem. A* **1997**, *101*, 7426.
(13) Tsuzuki, S.; Uchimaru; T.; Matsumura, M.; Mikami, M.; Tanabe, K. *J. Chem. Phys.* **1999**, *110*, 2858.
(14) Arulmozhiraja, A.; Fujii, T. *J. Chem. Phys.* **2001**, *115*, 10589.
(15) Fabiano, E.; Della Sala, F. *Chem. Phys. Lett.* **2006**, *418*, 496.
(16) Rubio, M; Merchan, M; Orti, E.; Roos, B. O. *Chem. Phys. Lett.* **1995**, *234*, 373.
(17) Almenningen, A.; Bastiansen, O.; Fernholt, L.; Cyvin, B. N.; Cyvin, S. J.; Samdal, S. *J. Mol. Struct. (Theochem)* **1985**, *128*, 59.
(18) Charbonneau, G. P.; Delugeard, Y. *Acta Crystallogr., Sect. B* **1976**, *32*, 1420.
(19) Baudour, J. L.; Toupet, L.; Delugeard, Y.; Ghemid, S. *J. Acta Crystallogr., Sect. C* **1986**, *42*, 1211.
(20) Delugeard, Y. *Acta Crystallogr., Sect. B* **1976**, *32*, 702.
(21) Baker, K. N.; Fratini, A. V.; Resch, T.; Knachel, H. C.; Adams, W. W.; Socci, E. P.; Farmer, B. L. *Polymer* **1993**, *34*, 1571.
(22) Matsuoka, S.; Fujii, H.; Yamada, T.; Pac, C.; Ishida, A. *J. Phys. Chem.* **1991**, *95*, 5802.
(23) Mabbs, R.; Nijegorodov, N.; Downey, W. S. *Spectrochim. Acta, Part A* **2003**, *59*, 1329.
(24) Bouzakraoui, S.; Bouzzine, S. M.; Bouchrine, M.; Hamidi, M. *J. Mol. Struct. (Theochem)* **2005**, *725*, 39.
(25) Heimel, G.; Daghofer, M.; Gierschner, J.; List, E. J. W.; Grimsdale, A. C.; Müllen, K.; Belojonne, D.; Brédas, J.-L; Zojer, E. *J. Chem. Phys.* **2005**, *122*, 54501.
(26) Furche, F.; Ahlrichs, R. *J. Chem. Phys.* **2002**, *117*, 7433.
(27) Christiansen, O.; Koch, H.; Jørgensen, P. *Chem. Phys. Lett.* **1995**, *243*, 409.
(28) Köhn, A.; Hättig, C. *J. Chem. Phys.* **2003**, *119*, 5021.
(29) Hättig, C. *J. Chem. Phys.* **2003**, *118*, 7751.
(30) Lukeš, V.; Aquino, A.; Lischka, H. *J. Phys. Chem. A* **2005**, *109*, 10232.
(31) Beenken, W. J. D.; Lischka, H. *J. Chem. Phys.* **2005**, *123*, 144311.
(32) Bauernschmitt, R.; Ahlrichs, R. *Chem. Phys. Lett.* **1996**, *256*, 454.
(33) Bauernschmitt, R.; Häser, M.; Treutler, O.; Ahlrichs, R. *Chem. Phys. Lett.* **1997**, *264*, 573.
(34) Becke, A. D. *J. Chem. Phys.* **1993**, *98*, 5648.

(35) Zerner, M. C.; Loew, G. H.; Kirchner, R. F.; Mueller-Westerhoff, U. T. *J. Am. Chem. Soc.***1980**, *102*, 589.
(36) Schäfer, A.; Horn, H.; Ahlrichs, R. *J. Chem. Phys.* **1992**, *97*, 2571.
(37) Schäfer, A.; Huber, C.; Ahlrichs, R. *J. Chem. Phys.* **1994**, *100*, 5829.
(38) Ahlrichs, R.; Bär, M.; Häser, M.; Horn, H.; Kölmel, C. *Chem. Phys. Lett.* **1989**, *162*, 165.
(39) *HYPERCHEM*, rel. 7.5 for Windows, Hypercube, Inc., 2003.
(40) Ma, J.; Li, S.; Jiang, Y. *Macromol.* **2002**, *35*, 1109.
(41) Yang, L.; Feng, J. K.; Ren, A. M. *J. Mol. Struct. (Theochem*) **2006**, *758*, 29.
(42) Fabiano, E.; Della Salla, F.; Cingolani, R.; Weimer, M.; Görling, A. *J. Phys. Chem. A* **2005**, *109*, 3078.
(43) Artacho, E.; Rohlfing, M.; Côté, M.; Haynes, P. D.; Needs, R. J.; Molteni, C. *Phys Rev. Lett.* **2004**, *93*, 116401.
(44) Brandsen, B. H.; Joachain, C. J. *Physics of Atoms and Molecules*; Longman Group Limited: London, 1983.
(45) Sancho-Garcia, J. C.; Cornil, J. *J. Chem. Theory Comput.* **2005**, *1*, 581.
(46) Im, H.-S.; Bernstein, E. R. *J. Chem. Phys.* **1988**, *88*, 7337. This paper contains an error in eq 2, which calls for a correction according to ref 31.